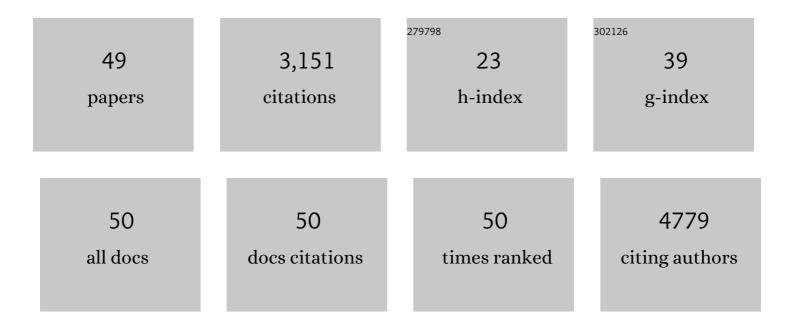


List of Publications by Year in descending order

Source: https://exaly.com/author-pdf/4129701/publications.pdf Version: 2024-02-01



| # | Article | IF | CITATIONS |
|----|--|------|-----------|
| 1 | Study of the interfacial adhesion properties of a novel Self-healable siloxane polymer material via molecular dynamics simulation. Applied Surface Science, 2022, 583, 152471. | 6.1 | 3 |
| 2 | Effect of hydrogen bonds on the thermal transport in a precisely branched polyethylene with ordered and amorphous structures. Computational Materials Science, 2022, 205, 111191. | 3.0 | 5 |
| 3 | Role of water environment in chemical degradation of a covalent organic framework tethered with quaternary ammonium for anion exchange membranes. RSC Advances, 2022, 12, 19240-19245. | 3.6 | 1 |
| 4 | The Influence of Properties of Solder Joint on the Stress of Underfill in Flip Chip Package. , 2022, , . | | 0 |
| 5 | Mold Flow Simulation Analysis of Molded Underfill in an Ultra-thin High-Density Package. , 2022, , . | | 3 |
| 6 | Ultrahigh-Aspect-Ratio Boron Nitride Nanosheets Leading to Superhigh In-Plane Thermal Conductivity of Foldable Heat Spreader. ACS Nano, 2021, 15, 6489-6498. | 14.6 | 191 |
| 7 | Numerical homogenization of thermal conductivity of particle-filled thermal interface material by fast Fourier transform method. Nanotechnology, 2021, 32, 265708. | 2.6 | 13 |
| 8 | Soft and Selfâ€Adhesive Thermal Interface Materials Based on Vertically Aligned, Covalently Bonded Graphene Nanowalls for Efficient Microelectronic Cooling. Advanced Functional Materials, 2021, 31, 2104062. | 14.9 | 95 |
| 9 | A comprehensive study of pyrazine-contained and low-temperature curable polyimide. Polymer, 2021, 228, 123963. | 3.8 | 23 |
| 10 | The Effect of Thermal-Induced Warpage and Degeneration of Thermal Interface Materials on the Thermal Performance of a Flip-Chip Package. , 2021, , . | | 1 |
| 11 | Comparison between two numerical methods for the computation of thermal conductivities of particulate composites: FEM and GeoDict. , 2021, , . | | 0 |
| 12 | Comparative Analysis of Temperature-induced Micro-scale Deformation of Package by Experiment and Finite Element Analysis. , 2021, , . | | 3 |
| 13 | Numerical analysis of the microscopic factors influencing the thermal conductivity of Al2O3/ AIN polymer composites. , 2021, , . | | 0 |
| 14 | Orthogonal Experiment for Analyzing the Impact of Thermal Stress on the Reliability of an EMC Package. , 2021, , . | | 0 |
| 15 | Characterization and Verification of Viscoelastic Constitutive Parameters of Underfill Material. , 2021, , . | | 5 |
| 16 | Viscoelastic Characterization and Simulation of Thermal Interface Materials. , 2021, , . | | 3 |
| 17 | Numerical analysis on the effect of microstructures on the thermal and mechanical properties of carbon fiber / Al2O3 thermal pad. , 2021, , . | | 0 |
| 18 | Mechanism of Facilitation of Ion Mobility in Low-Water-Content Fuel Cell Membranes. Journal of Physical Chemistry C, 2021, 125, 27703-27713. | 3.1 | 12 |

Jibao Lu

| # | Article | IF | CITATIONS |
|----|--|------|-----------|
| 19 | Width and Clustering of Ion-Conducting Channels in Fuel Cell Membranes Are Insensitive to the Length of Ion Tethers. Journal of Physical Chemistry C, 2021, 125, 27693-27702. | 3.1 | 11 |
| 20 | Facile and Efficient Welding of Silver Nanowires Based on UVAâ€Induced Nanoscale Photothermal Process for Rollâ€ŧoâ€Roll Manufacturing of Highâ€Performance Transparent Conducting Films. Advanced Materials Interfaces, 2019, 6, 1801635. | 3.7 | 30 |
| 21 | Suppressing Photoinduced Charge Recombination via the Lorentz Force in a Photocatalytic System. Advanced Science, 2019, 6, 1901244. | 11.2 | 101 |
| 22 | Effect of Polymer Architecture on the Nanophase Segregation, Ionic Conductivity, and Electro-Osmotic Drag of Anion Exchange Membranes. Journal of Physical Chemistry C, 2019, 123, 8717-8726. | 3.1 | 35 |
| 23 | A Paper-Like Inorganic Thermal Interface Material Composed of Hierarchically Structured Graphene/Silicon Carbide Nanorods. ACS Nano, 2019, 13, 1547-1554. | 14.6 | 131 |
| 24 | 3D interconnected high aspect ratio tellurium nanowires in epoxy nanocomposites: serving as thermal conductive expressway. Journal of Applied Polymer Science, 2019, 136, 47054. | 2.6 | 17 |
| 25 | Enhanced thermal conductivity for Ag-deposited alumina sphere/epoxy resin composites through manipulating interfacial thermal resistance. Composites Part A: Applied Science and Manufacturing, 2018, 107, 561-569. | 7.6 | 115 |
| 26 | Multiscale Modeling of Structure, Transport and Reactivity in Alkaline Fuel Cell Membranes: Combined Coarse-Grained, Atomistic and Reactive Molecular Dynamics Simulations. Polymers, 2018, 10, 1289. | 4.5 | 26 |
| 27 | Effect of chemical functionalization on the thermal conductivity of 2D hexagonal boron nitride. Applied Physics Letters, 2018, 113, . | 3.3 | 43 |
| 28 | Improving thermal conductivity of polymer composites by reducing interfacial thermal resistance between boron nitride nanotubes. Composites Science and Technology, 2018, 165, 322-330. | 7.8 | 98 |
| 29 | Parameterization of a coarse-grained model with short-ranged interactions for modeling fuel cell membranes with controlled water uptake. Physical Chemistry Chemical Physics, 2017, 19, 17698-17707. | 2.8 | 20 |
| 30 | High-Resolution Coarse-Grained Model of Hydrated Anion-Exchange Membranes that Accounts for Hydrophobic and Ionic Interactions through Short-Ranged Potentials. Journal of Chemical Theory and Computation, 2017, 13, 245-264. | 5.3 | 31 |
| 31 | Relationship between the line of density anomaly and the lines of melting, crystallization, cavitation, and liquid spinodal in coarse-grained water models. Journal of Chemical Physics, 2016, 144, 234507. | 3.0 | 32 |
| 32 | Modeling Molecular Interactions in Water: From Pairwise to Many-Body Potential Energy Functions. Chemical Reviews, 2016, 116, 7501-7528. | 47.7 | 314 |
| 33 | Coarse-Graining of TIP4P/2005, TIP4P-Ew, SPC/E, and TIP3P to Monatomic Anisotropic Water Models Using Relative Entropy Minimization. Journal of Chemical Theory and Computation, 2014, 10, 4104-4120. | 5.3 | 108 |
| 34 | N- and Mo-doping Bi2WO6 in photocatalytic water splitting. Computational Materials Science, 2013, 67, 88-92. | 3.0 | 39 |
| 35 | Synergistic effects of codopants on photocatalytic O2 evolution in BiVO4. Solid State Sciences, 2013, 24, 79-84. | 3.2 | 20 |
| 36 | Effect of Electronegativity and Charge Balance on the Visible-Light-Responsive Photocatalytic Activity of Nonmetal Doped Anatase TiO _{2. International Journal of Photoenergy, 2012, 2012, 1-8.} | 2.5 | 22 |

Jibao Lu

| # | Article | IF | CITATIONS |
|----|---|-----|-----------|
| 37 | Topological phase transition and unexpected mass acquisition of Dirac fermion in TlBi(S1â^xSex)2. Applied Physics Letters, 2012, 101, 182101. | 3.3 | 6 |
| 38 | The Synthetic Effects of Iron with Sulfur and Fluorine on Photoabsorption and Photocatalytic Performance in Codoped. International Journal of Photoenergy, 2012, 2012, 1-7. | 2.5 | 2 |
| 39 | Chemical and optical properties of carbon-doped TiO2: A density-functional study. Applied Physics Letters, 2012, 100, 102114. | 3.3 | 54 |
| 40 | Tuning of the Surface-Exposing and Photocatalytic Activity for AgX (X = Cl and Br): A Theoretical Study. Journal of Physical Chemistry C, 2012, 116, 19372-19378. | 3.1 | 31 |
| 41 | Hydrogenated titania: synergy of surface modification and morphology improvement for enhanced photocatalytic activity. Chemical Communications, 2012, 48, 5733. | 4.1 | 285 |
| 42 | Structure and Electronic Properties and Phase Stabilities of the Cd _{1â^^<i>x</i>} Zn _{<i>x</i>} S Solid Solution in the Range of O≤i>xâ‰\$. ChemPhysChem, 2012, 13, 147-154. | 2.1 | 21 |
| 43 | Effective increasing of optical absorption and energy conversion efficiency of anatase TiO2 nanocrystals by hydrogenation. Physical Chemistry Chemical Physics, 2011, 13, 18063. | 2.8 | 92 |
| 44 | Density Functional Characterization of Pure and Alkaline Earth Metalâ€Doped Bi ₁₂ GeO ₂₀ , Bi ₁₂ SiO ₂₀ , and Bi ₁₂ TiO ₂₀ Photocatalysts. ChemCatChem, 2011, 3, 378-385. | 3.7 | 21 |
| 45 | Electronic and magnetic properties of perfect, vacancy-doped, and nonmetal adsorbed MoSe2, MoTe2 and WS2 monolayers. Physical Chemistry Chemical Physics, 2011, 13, 15546. | 2.8 | 428 |
| 46 | Composition Dependence of the Photocatalytic Activities of BiOCl _{1â^^<i>x</i>} Br _{<i>x</i>} Solid Solutions under Visible Light. Chemistry - A European Journal, 2011, 17, 9342-9349. | 3.3 | 196 |
| 47 | Hierarchical TiO ₂ Microspheres: Synergetic Effect of {001} and {101} Facets for Enhanced Photocatalytic Activity. Chemistry - A European Journal, 2011, 17, 15032-15038. | 3.3 | 180 |
| 48 | First-principles study of the electronic and magnetic properties of oxygen-deficient rutile TiO2(110) surface. Journal of Solid State Chemistry, 2011, 184, 1148-1152. | 2.9 | 23 |
| 49 | Synergistic effect of crystal and electronic structures on the visible-light-driven photocatalytic performances of Bi2O3 polymorphs. Physical Chemistry Chemical Physics, 2010, 12, 15468. | 2.8 | 261 |